Spectrum of Engineering Sciences
ISSN (e) 3007-3138 (p) 3007-312X Volume 3, Issue 8, 2025

OPTIMIZING FVD ORIENTATIONS FOR TALL RC BUILDINGS UNDER COMBINED SEISMIC & WIND HAZARDS

Umer Shahzad [1,a], Ahmed Saboor [1,b], M. Adil Javaid [1, c], Farah Naz[1 d], Naveed Anjum [1,e] Tamjeed Attaullah [1,f], Muhammad Ali [1,g], Usama Afzal [1,h] , Zaheer Ahmed [1,i]

[1]Khawaja Fareed University of Engineering & Information Technology (KFUEIT), Rahim Yar Khan, Pakistan

[a] umer.shahzad@kfueit.edu.pk, [b]ahmedsaboor2003@gmail.com, [c]m.adiljaved2@gmail.com, [d]farah.naz@kfueit.edu.pk [e]naveed.anjum@kfueit.edu.pk, [f]muhammadtamjeed26@gmail.com, [g]muhammadali5552237@gmail.com, [h]afzalusama54@gmail.com, , [i]dr.zaheer@kfueit.edu.pk

Keywords (Fluid viscous dampers; reinforced-concrete frame; nonlinear time-history analysis; inter-storey drift; seismic energy dissipation; wind-seismic interaction)

Article History
Received on 08 July 2025
Accepted on 25 July 2025
Published on 19 August 2025

Corresponding Author: *
Umer Shahzad

Abstract

A 20-storey reinforced-concrete frame (designed per ACI 318-19, ASCE 7-16 and local BCP-21 codes) is analyzed under nonlinear time-history seismic loads (using spectrally matched ground motions) and ASCE wind loading for a Karachi like coast. Three supplemental fluid viscous damper (FVD) layouts are studied: single diagonal braces, chevron bracing, and wall mounted dampers. Compared to the bare frame, all damper configurations yield substantial improvements in dynamic response. Under the design seismic sequences, the wall-mounted dampers provide the strongest control: peak inter-storey drift is cut by about 42% (to ~0.00618) and roof displacement by roughly 50%, while ~58.6% of the input seismic energy is dissipated by the system. The chevron arrangement also significantly reduces response, absorbing about 42.1% of the energy, and the single diagonal layout about 36.8%. In absolute terms these devices roughly halve the undamped building's drifts and displacements across height. Under wind excitation, the trends differ: chevron or diagonal orientations better suppress low-frequency sway, whereas the wall-mounted scheme maximizes energy dissipation and drift control under earthquake shaking. These results highlight a tradeoff in mixed hazards. For a high-wind, high-seismic site like coastal Karachi, a hybrid strategy is advised: e.g., chevron dampers on the windward facade to counter aerodynamic sway, combined with dense wall mounted dampers on the transverse axis for optimal seismic energy dissipation. Such damper layouts provide actionable guidance for resilient tall building design under combined seismic and wind loads.

INTRODUCTION

1. Introduction

Today, high rise buildings have become very significant in city development since they offer solutions to the scarce availability of land space and yet contain the growing population density [1]. Nevertheless, they are more susceptible to dynamic loads and mostly those that result because of an earthquake due to their large height and slenderness [2]. The structural response under seismic loads of the tall buildings is not determined by the stiffness and strength of the building only, but also by the efficiency of the energy dissipating capacity of the building. Commonly used seismic design methods are aiming to enhance the strength and ductility but such methods can have economical and architectural limitations. As a result, the inclusion of supplemental damping systems has emerged as an attractive feasible means of enhancing the seismic by removing the need to compromise flexibility in architecture [3,4].

The working principle of fluid viscous dampers is to absorb the seismic energy by controlling sliding of a piston in a cylinder containing a viscous fluid and dampen the vibrations of the structure [5]. Such devices are also effective at a broad frequency range, and do not rely on displacement amplitude, thus making them applicable in retrofit, as well as on new constructions [6]. During the last several decades, the evolution of performance -based seismic design made the role of supplemental damping systems in tall buildings reinforced [7,8]. FVDs are an example of the various passive energy dissipation systems that are quite efficient, reliable and can be placed in different ways, including, single diagonal, chevron, and toggle-brace arrangements [9].

This is because the direction and arrangement of FVDs in the structural system has a considerable implication on the performance of reduce seismic response [10]. Single diagonally bracing has direct energy dissipation and can potentially cause localized concentrators of openings. Distribution of force can be enhanced in Chevron arrangements, which will change the drift patterns and the system of toggle-brace enhances energy dissipation capacity due to the amplified damper stroke [11]. Experimental and numerical analysis presented that inter-storey drift, base shear and energy dissipation efficiency are also influenced by the selection of damper type [12,13]. Although positive progress has been realized in these regards, majority of the work has been based on optimization of damper characteristics or investigation of a particular orientation without in-depth comparison studies of various orientations in tall reinforced concrete (RC) buildings [14].

When the site is prone to the earthquake, the high-rise building must be designed to be serviceable and safe on the event of frequent and exceptional earthquake. With evolutions in the levels of seismic hazards and the building codes, it becomes more and more important to know how lies the orientation of FVD on the global and local seismic performance measures [15]. By combining analytical modeling with design processes employing codes, more thorough analysis can be included in cases where the real-world

loading conditions are considered, and an optimized performance of a kind that fits within current resiliency-based design philosophies can be achieved.

Albeit the established benefits of fluid viscous dampers, there still exists a dearth of thorough study regarding comparative seismic performance of various damper orientations on high-rise RC. This research fills this gap with an analysis of a 20-storey RC structure fitted with FVDs in single diagonal, chevron and Wall Mounted arrangements. The structure is modeled based on the provisions of ACI 318-19 [5], ASCE 7-16 [6], and applied to the ground motions that characterize the local seismic. The main performance measures such as top-storey drift, base shear, and cumulative energy dissipation are estimated to ascertain the most successful positioning of the seismic resilience. The results of this study are intended to offer viable recommendations to engineers and architects on the best way to design the envisaged FVDs to facilitate the safety and serviceability of high-rise buildings in earthquake prone areas.

Even though fluid viscous dampers have demonstrated admirable benefits, there is still a gap in the systematic study in evaluating the comparative seismic performance of various damper orientation in high-rise RC building. This paper answers this gap working on a 20-storey RC building model with FVDs mounted in single diagonal, chevron, and toggle-brace formations. The building can be categorized as a structure that will be designed in accordance with the ACI 318-19 [16], and ASCE 7-16 [17] stipulations and that will be exposed to ground motions representative of local seismicity during a design earthquake. The top-storey drift, base shear, and cumulative energy dissipation performance parameters are used to define the best orientation, that makes a structure seismic resilient. The results of this study would give real life advice to engineers and designers regarding the best FVD workings in a far more satisfactory construction of tall buildings in earthquake prone areas.

2. Research Methodology

2.1 Overview of Study Phase:

The methodology for this research unfolds in five distinct but interrelated phases.

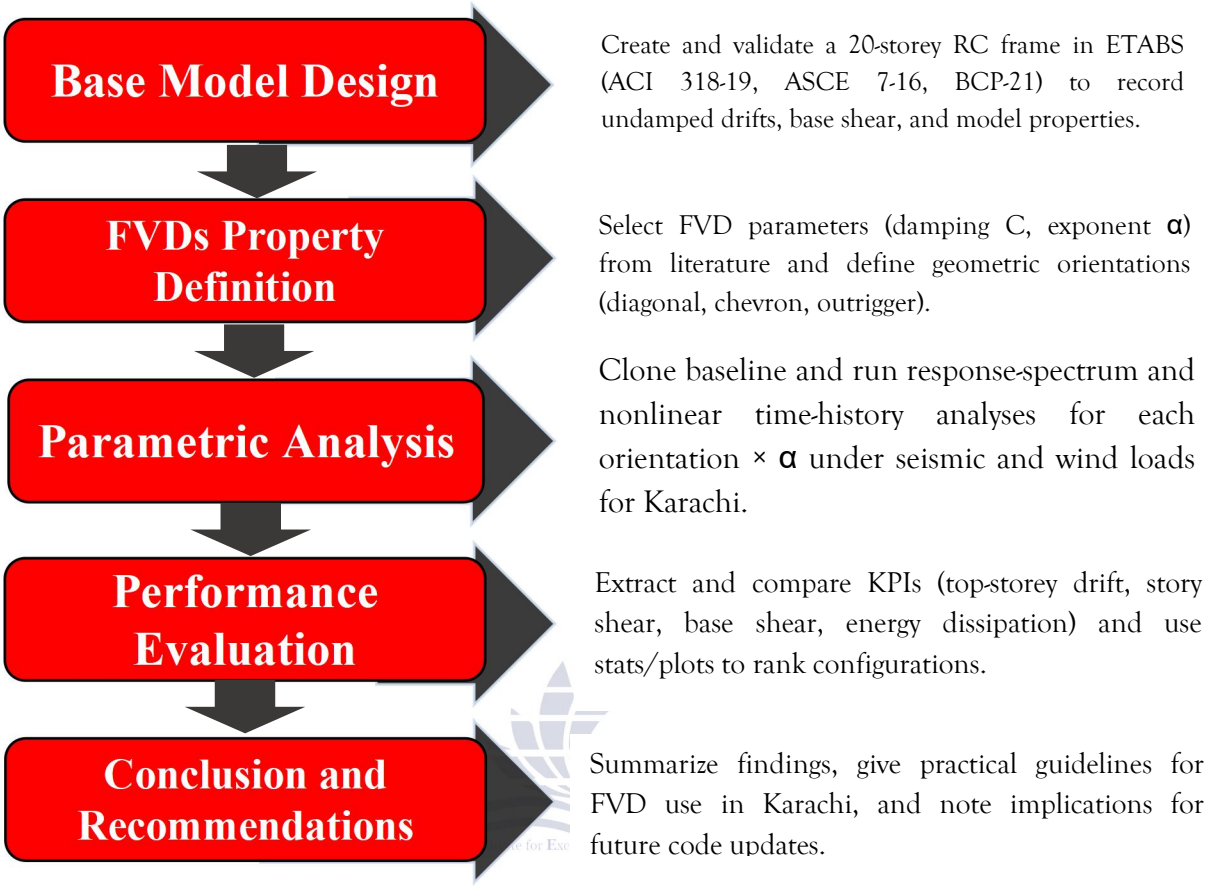

Figure 2.1: Flowchart of Methodological Steps

2.2 Building Geometry and Structural Properties:

2.2.1 Description of the 20-Storey RC Frame:

The 20-story frame is composed of moment-resisting beams and columns forming a grid in each principal direction. Typical beam sizes might range from about 300×600 mm at the lower levels to ~300×450 mm at upper levels, and column sizes might range from about 800×800 mm at the base to 500×500 mm at the top (exact sizes depend on design). These members are reinforced concrete; for example, A 20-story RC frame using 250×300 mm beams and 450×450 mm columns with 150 mm floor slabs. Shear walls are placed around cores to enhance stiffness. The floor diaphragms (slabs) tie the frame together. Vertical circulation cores and stairwells are typically stiffened by shear walls. It has a typical story height of 3.657 m per floor for first 10 floors, 3.048m for the rest of the floors and a base height of 3.81m, giving a total height on the order of 67.056 m. The model labels element sections with prefixes (e.g., "C" for columns, "F" for floor beams) for clarity. Live load and wall dead load were assigned to each story (e.g. 3 kN/m² live plus wall weight). Gravity and lateral loads (wind and seismic in two orthogonal directions) were applied per code. The result is a stiff, high-rise concrete frame

suitable for typical office or residential use in a moderate seismic region.

2.3 Code Selection and Load Definition:

The design and analysis follow the latest building and load codes. The building code of Pakistan 2021 (BCP-2021) is now the governing standard, which adopts international provisions. BCP-2021 is based on the 2021 International Building Code (IBC-2021) and references ASCE/SEI 7-16 for loads and ACI 318-19 for concrete design. In concrete design, ACI 318-19 ("Building Code Requirements for Structural Concrete") provides all requirements for member strength and detailing. ASCE 7-16 defines gravity, wind, and seismic load criteria. Thus, the model uses ACI 318-19 for material and detail specifications, ASCE 7-16 for load determinations, and BCP-21 to unify these.

1 Seismic Design Parameters

The seismic design criteria for Karachi are established in accordance with the ASCE 7-16 provisions, as formally adopted by the Building Code of Pakistan 2021 (BCP-21).

2.3.2 Design Response Spectrum:

$T_a = C_t h_n^x$ $C_t = 0.016$, $x = 0.90$

2.3.3 Mapped Accelerations:

S_s = 0.82 g (short-period, 0.2 s)

S_1 = 0.32 g (1.0 s)

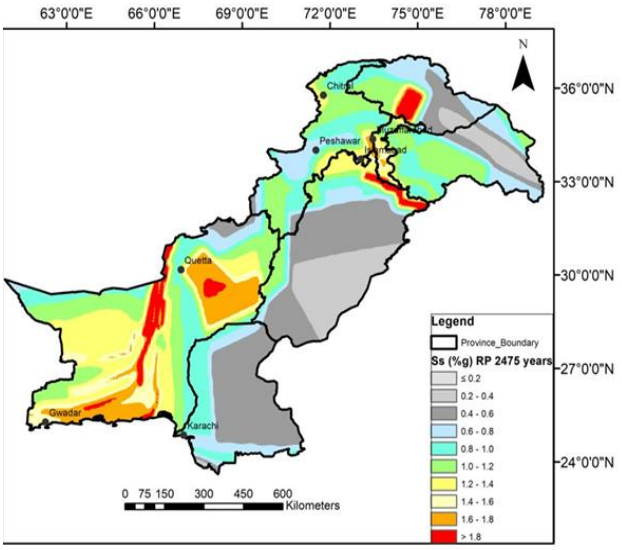

Figure 2.2: 0.2-sec Spectral Accel. (BCP-21: figure 1613.2.1(1))

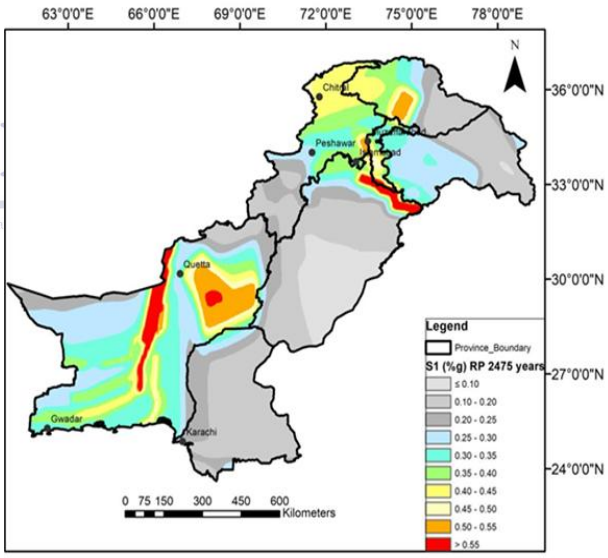

Figure 2.3: 1-sec Spectral Accel. (BCP-21: figure 1613.2.1(2))

2.3.4 Soil & Site Coefficients:

Site Class E (soft clay)

Fa = 1.2, Fv = 2.72 (ASCE 7-16 Ch 11 Table 11.4-2, based on Site Class E)

2.3.5 Frame Factors (ASCE 7-16: Table12.2-1(Continued)):

R = 8 (Response modification)

Ω_0 = 3 (Overstrength)

C_d = 5.5 (Deflection amplification)

I = 1.0 (Importance)

2.3.6 Wind Design Parameters

Wind loads follow ASCE 7-16 as referenced by BCP-21:
Basic Wind Speed: V = 120 mph (3-s gust) (BCP-21: 1609.3 Basic design wind speed)
Exposure Category: C (ASCE 7-16: 26.7.3 Exposure Categories)
Gust and Directionality Factors:
G = 0.85

K_d = 0.85 (ASCE 7-16: Table 26.6-1)

K_{zt} = 1.0 (ASCE 7-16: figure 26.8-1)

K_z (ASCE 7-16: Table26.10-1)

2.4 Parameters from Damper Design Manual (Taylor Devices et al.):

Parameters from Taylor Devices' Damper Design Manual, ("Damper Output Characteristics & Unique Benefits"), include the mass, self-weight, nominal damping coefficient (C) at 1 m/s, Damping Exponent (α = 0.4), stroke capacity, and continuous force rating for the models. These figures underpin the nonlinear link properties defined in ETABS.

US Units Kip-(s/in)$^{0.4}$	Metric Units kN-(s/m)$^{0.4}$	MKS Units Tonf-(s/m)$^{0.4}$
23	439	45
26	504	51
30	580	59
35	677	69
30	773	79
46	889	91

3. Results & Discussion

3.1 Overview:

The numerical and graphical results of nonlinear analyses carried out on the 20-storey reinforced-concrete building with fluid viscous dampers (FVDs). Results are organized by Total Damping Power (80,000 kN.s/m) equivalent. For each combination the following outputs are presented and compared against the baseline (no-damper) model: maximum story displacement, maximum inter-story drift ratio, representative hysteresis loops, and cumulative energy dissipated by the dampers. All nonlinear time-history analyses use spectrally matched ground motions and the Fast Nonlinear Analysis (FNA) procedure. Results are reported in SI units and drift ratios are given as decimals and percentages. Primary response metrics are (a) maximum story displacement (mm), (b) maximum inter-story drift ratio (decimal and %), (c) representative hysteresis loops (force vs. relative displacement) for selected dampers, and (d) cumulative energy dissipated by the dampers (kN-m).

3.2 Undamped Model:

The maximum displacement of the model without damper for RS-TH Load Case was: 301.4mm along x-axis and 509.4mm along y-axis. Total model height is 67670 mm. According to ASCE 7-16 the max allowed storey displacement id 2% of total height.

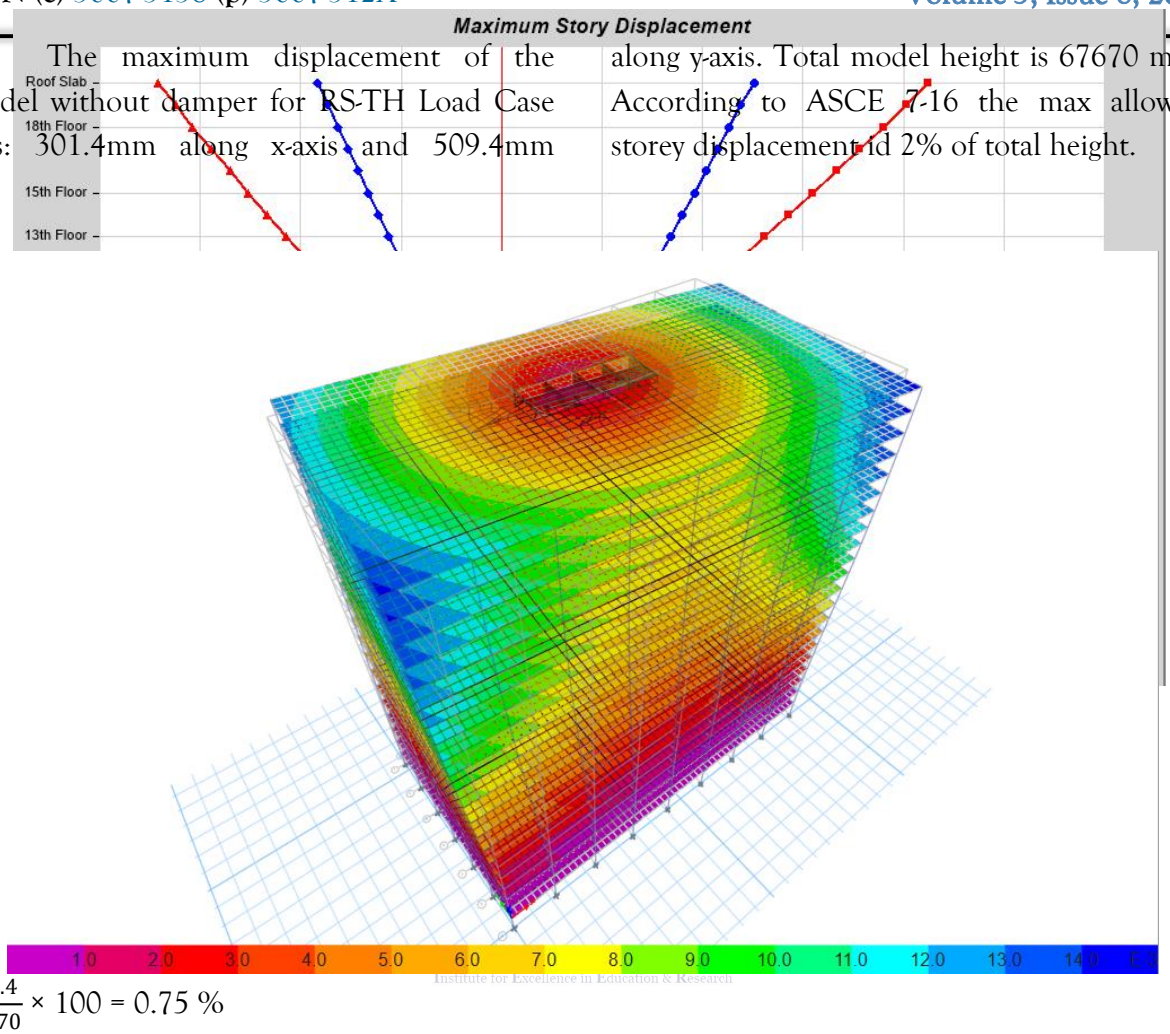

$$\frac{509.4}{67670} \times 100 = 0.75\ \%$$

Figure 3.1: Undamped Model Deformed Shape for Load Case RS-TH

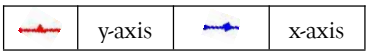

Figure 3.2: Undamped model Storey Displacement

Table 3.1: Undamped model Max and Min Storey displacements for RS-TH

Storey	Elevation	X-Dir	Y-Dir	X-Dir Min	Y-Dir Min
	m	mm	mm	mm	mm
Roof Slab	67.67	301.41	509.48	-218.64	-410.52
19th Floor	64.62	285.57	483.12	-207.18	-389.65
18th Floor	61.57	271.43	455.87	-195.35	-369.25
17th Floor	58.52	258.28	427.94	-183.20	-346.95
16th Floor	55.47	244.53	399.76	-170.97	-324.23
15th Floor	52.43	230.23	371.40	-158.56	-301.98
14th Floor	49.38	215.77	342.69	-146.42	-279.58
13th Floor	46.33	201.13	314.47	-134.30	-257.28
12th Floor	43.28	186.49	286.25	-122.22	-234.87
11th Floor	40.23	171.61	258.28	-110.22	-212.42
10 Floor	36.58	156.38	230.69	-98.83	-190.19
9th Floor	32.92	138.41	198.53	-89.28	-165.97
8th Floor	29.26	120.25	172.48	-79.35	-141.70
7th Floor	25.60	103.20	145.39	-69.39	-118.16
6th Floor	21.95	88.25	117.97	-59.53	-95.89
5th Floor	18.29	72.88	91.37	-49.63	-74.67
4th Floor	14.63	58.05	66.96	-38.67	-55.35
3rd Floor	10.97	43.28	45.41	-27.93	-38.15
2nd Floor	7.32	28.87	27.97	-18.83	-25.09
1st Floor	3.66	15.75	14.13	-10.50	-13.51
Plinth	0.00	5.50	4.30	-3.50	-4.45
Base	-3.81	0	0	0	0

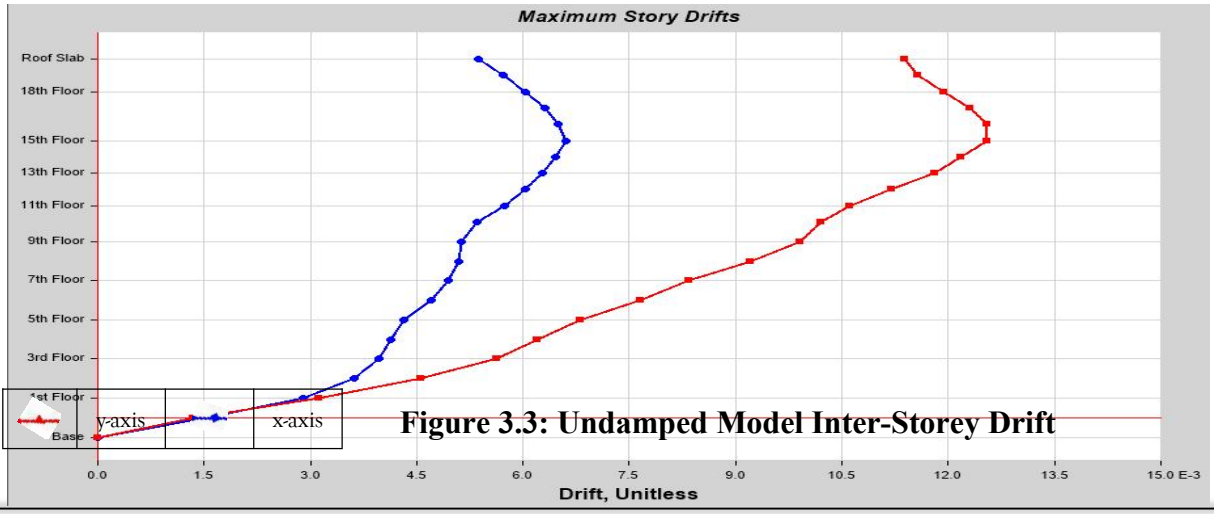

Figure 3.3: Undamped Model Inter-Storey Drift

Storey	Elevation	X-Dir	Y-Dir	Storey	Elevation	X-Dir	Y-Dir
	m				m		
Roof	67.67	0.00536	0.01139	Floor 9	32.92	0.00514	0.00991
Floor 19	64.62	0.00572	0.01157	Floor 8	29.26	0.00509	0.0092
Floor 18	61.57	0.00603	0.01194	Floor 7	25.60	0.00494	0.00834
Floor 17	58.52	0.00631	0.0123	Floor 6	21.95	0.0047	0.00765
Floor 16	55.47	0.00649	0.01255	Floor 5	18.29	0.00432	0.00682
Floor 15	52.43	0.00661	0.01255	Floor 4	14.63	0.00414	0.0062
Floor 14	49.38	0.00646	0.01218	Floor 3	10.97	0.00396	0.00562
Floor 13	46.33	0.00627	0.01181	Floor 2	7.32	0.00362	0.00455
Floor 12	43.28	0.00603	0.0112	Floor 1	3.66	0.0029	0.00313
Floor 11	40.23	0.00575	0.01061	Plinth	0.00	0.00151	0.00134
Floor 10	36.58	0.00536	0.01021	Base	-3.81	0	0

3.3 Model With Damping Power 80000 kN-s/m:

One Damper Force: 500 kN-s/m
Total no. of Damper: 120, Total Damping Force: 120 × 500 = 60000 kN-s/m

3.3.1 P. 80000kN-s/m Combination 1 (C1):

- 40 Viscous Dampers in Chevron Orientation applied on each side of the building from 5th to 16th Floor.
- C1's Max Storey Displacements are x-axis 303.67 mm and y-axis is 403.44 mm; Max inter-storey drift is 0.00961. Hysteresis plot is also acceptable.

Max Non-Linear Viscous Damping is 42.1%.

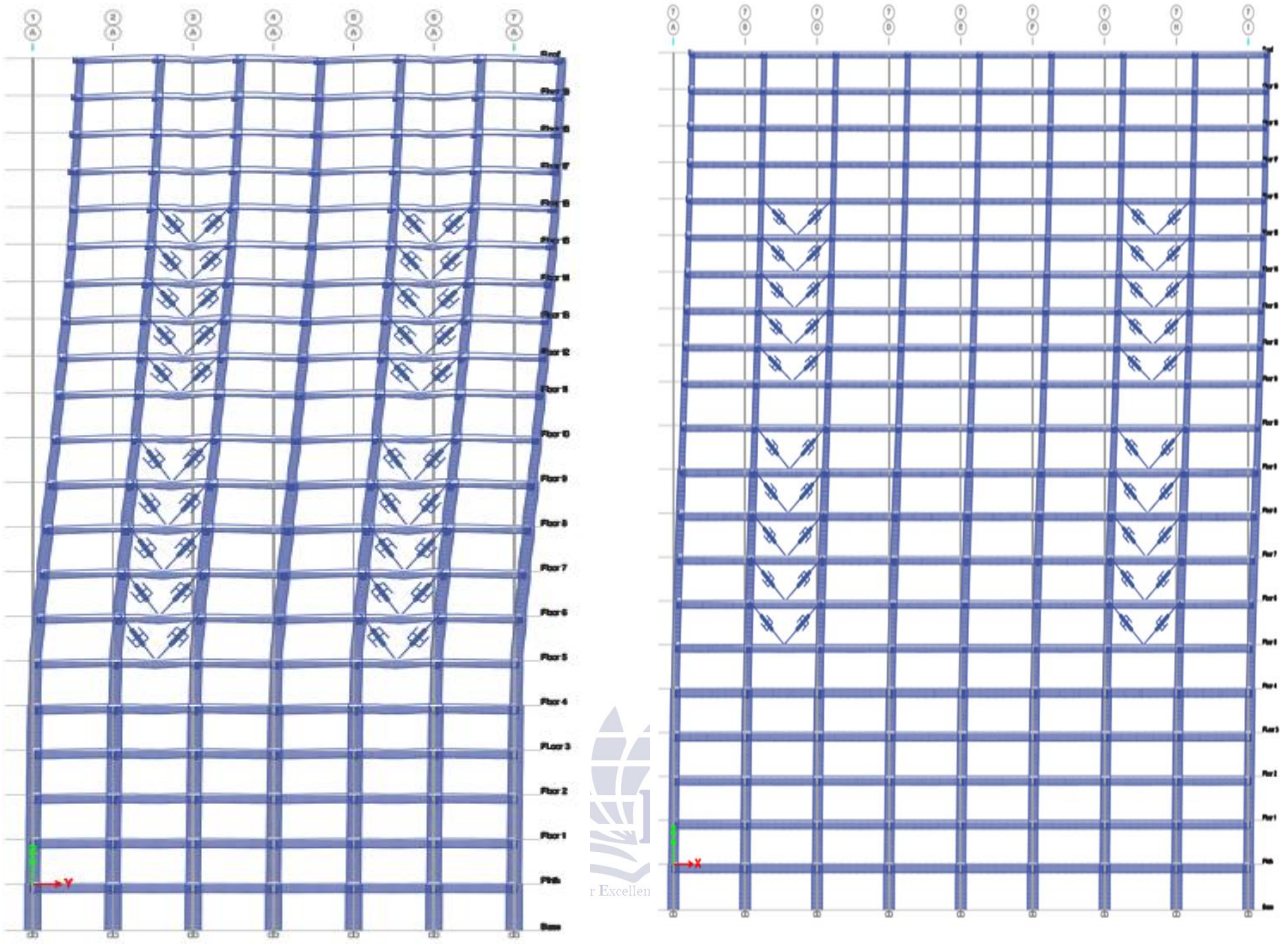

Figure 3.5: P 80000 kN-s/m C1 x-axis Deformed Shape

Figure 3.4: P 80000 kN-s/m C1 y-axis Deformed Shape

Table 3.3: P 80000 kN-s/m C1 Max and Min Storey Displacements for RS-TH

Storey	Elevation	X-Dir	Y-Dir	X-Dir Min	Y-Dir Min
	m	mm	mm	mm	mm
Roof	67.67	303.67	403.44	-210.83	-210.22
Floor 19	64.62	293.08	390.57	-201.98	-200.06
Floor 18	61.57	282.09	377.45	-192.78	-190.12
Floor 17	58.52	270.61	363.53	-183.33	-180.10
Floor 16	55.47	258.11	347.67	-173.64	-170.11
Floor 15	52.43	243.99	327.83	0.00	0.00
Floor 14	49.38	228.45	304.82	0.00	0.00
Floor 13	46.33	212.25	279.67	0.00	0.00
Floor 12	43.28	195.40	253.02	0.00	0.00
Floor 11	40.23	177.67	225.19	-119.60	-105.10
Floor 10	36.58	156.55	194.02	0.00	0.00

Floor 9	32.92	133.17	157.91	0.00	0.00
Floor 8	29.26	112.22	122.54	0.00	0.00
Floor 7	25.60	100.00	87.69	0.00	0.00
Floor 6	21.95	87.51	70.61	0.00	0.00
Floor 5	18.29	74.59	57.05	-38.44	-18.67
Floor 4	14.63	59.64	43.70	-27.83	-12.58
Floor 3	10.97	44.19	30.53	-20.19	-7.71
Floor 2	7.32	29.21	18.44	-13.85	-4.16
Floor 1	3.66	15.54	8.52	-8.40	-1.78
Plinth	0.00	4.87	2.18	-3.09	-0.43
Base	-3.81	0.00	0.00	0.00	0.00

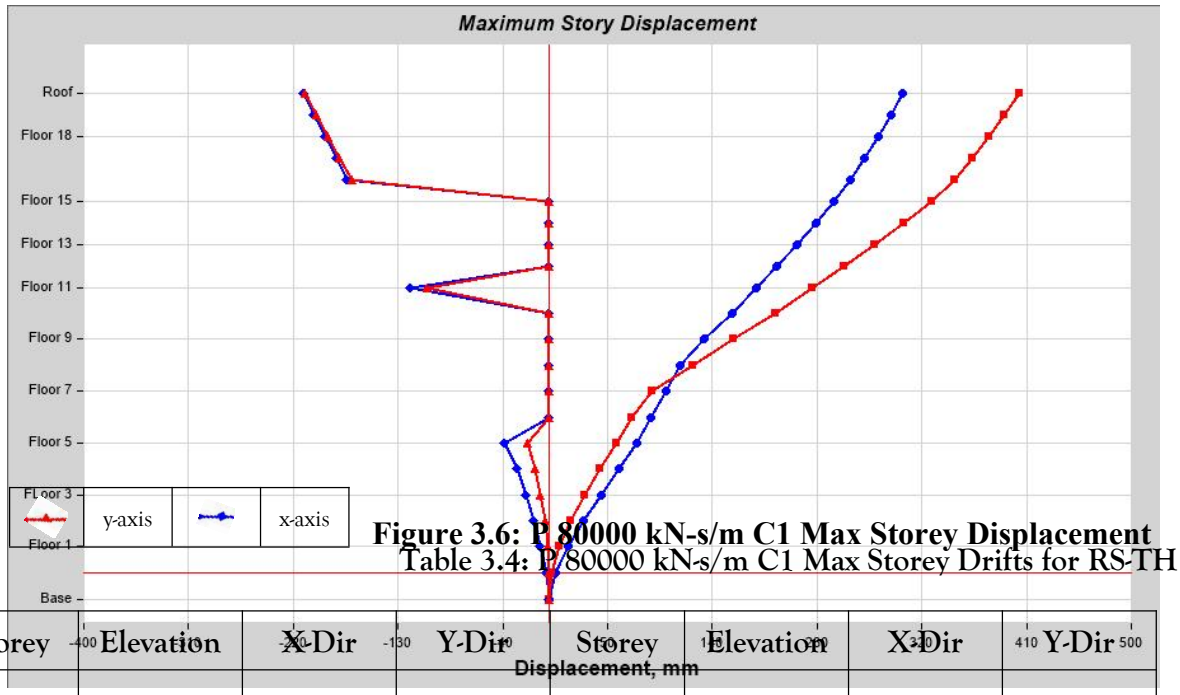

Figure 3.6: P 80000 kN-s/m C1 Max Storey Displacement

Table 3.4: P 80000 kN-s/m C1 Max Storey Drifts for RS-TH

Storey	Elevation	X-Dir	Y-Dir	Storey	Elevation	X-Dir	Y-Dir
	m				m		
Roof	67.67	0.003491	0.004813	Floor 9	32.92	0.006128	0.009894
Floor 19	64.62	0.00363	0.004922	Floor 8	29.26	0.006002	0.009615
Floor 18	61.57	0.003813	0.005217	Floor 7	25.60	0.005751	0.009154
Floor 17	58.52	0.004142	0.005933	Floor 6	21.95	0.005464	0.008532
Floor 16	55.47	0.004794	0.007526	Floor 5	18.29	0.004327	0.004961
Floor 15	52.43	0.005252	0.008107	Floor 4	14.63	0.004487	0.004748
Floor 14	49.38	0.0055	0.008416	Floor 3	10.97	0.004367	0.004236
Floor 13	46.33	0.005734	0.008966	Floor 2	7.32	0.003998	0.003392

Floor 12	43.28	0.005865	0.00961	Floor 1	3.66	0.00313	0.002136
Floor 11	40.23	0.005779	0.008878	Plinth	0.00	0.001374	0.000698
Floor 10	36.58	0.006391	0.010251	Base	-3.81	0	0

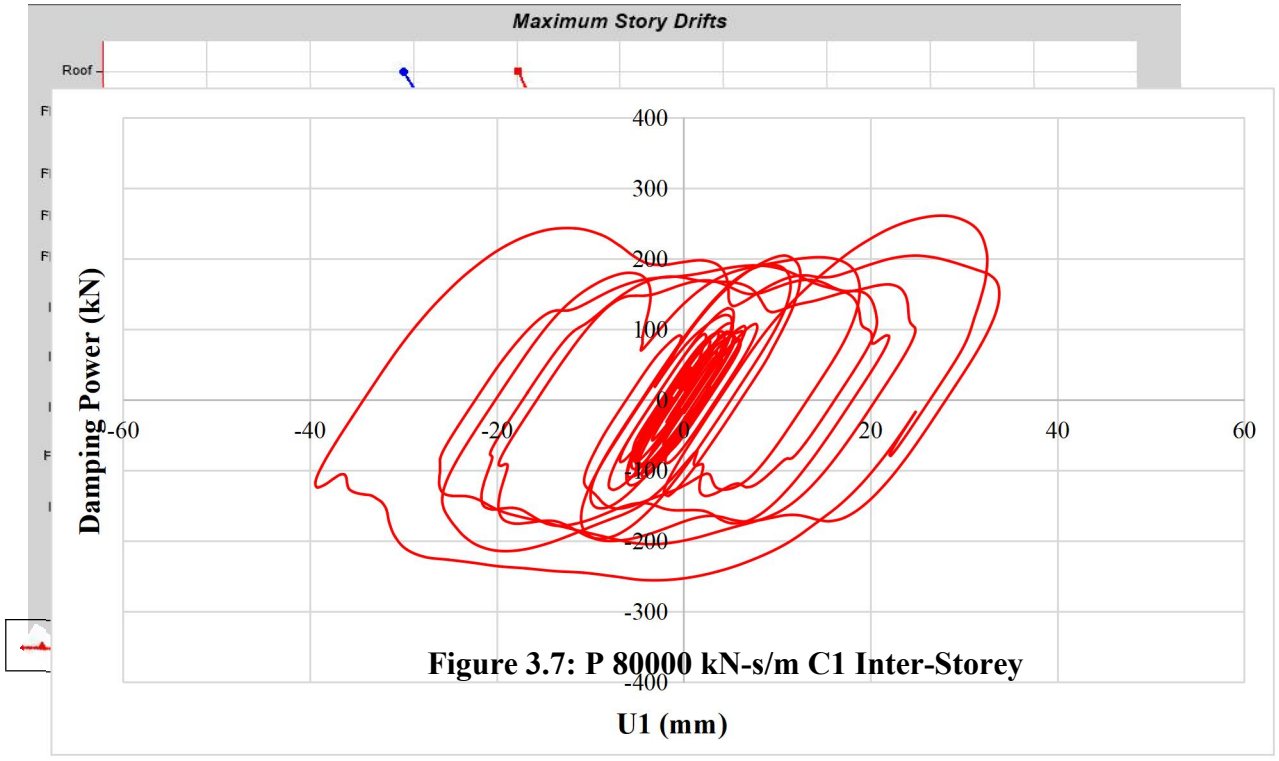

Figure 3.7: P 80000 kN-s/m C1 Inter-Storey

Figure 4.59: P 80000 kN-s/m C1 Inter-Storey Drift

Figure 3.8: P 80000 kN-s/m C1 Hysteresis Plot

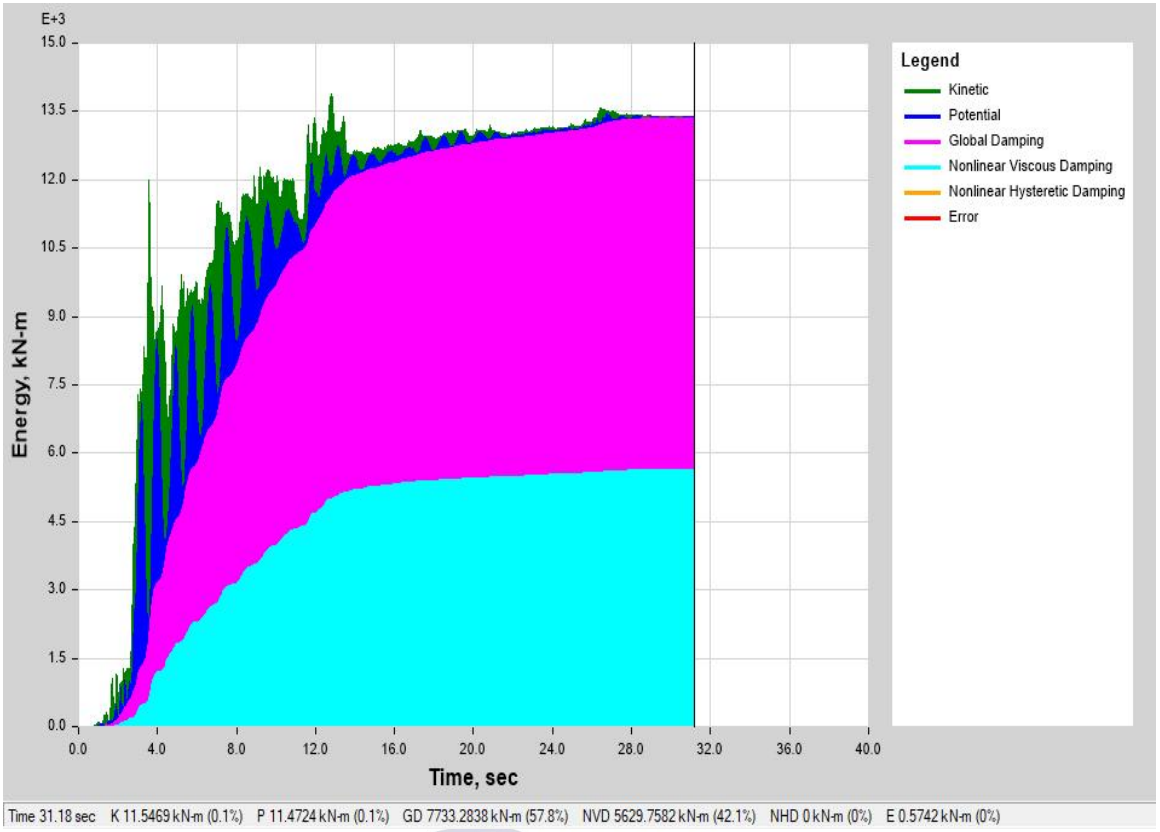

Figure 3.9: P 80000 kN-s/m C1 Cumulative Energy Plot

3.3.2 P. 80000kN-s/m Combination 2 (C2):

- 40 Viscous Dampers in Diagonal Orientation applied on each side of the building from Plinth to 20th Floor.
- C2's Max Storey Displacements are x-axis 290.41 mm and y-axis is 360.44 mm; Max inter-storey drift is 0.007163. Hysteresis plot is also acceptable.
- Max Non-Linear Viscous Damping is 36.8%.

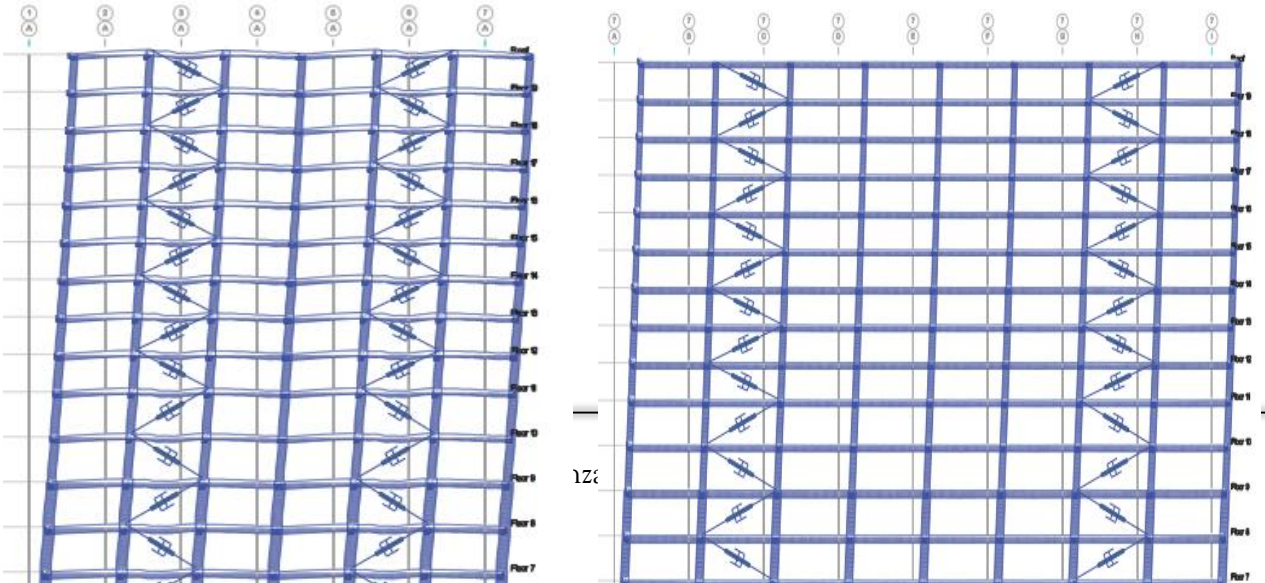

Table 3.5: P 80000 kN-s/m C1 Max Storey Drifts for RS-TH

Storey	Elevation	X-Dir	Y-Dir	X-Dir Min	Y-Dir Min
	m	mm	mm	mm	mm
Roof	67.67	290.41	360.44	-215.79	-227.05
Floor 19	64.62	280.86	348.58	-206.81	-213.04
Floor 18	61.57	270.69	336.18	-197.45	-198.98
Floor 17	58.52	259.98	323.22	-187.83	-185.33
Floor 16	55.47	248.57	309.55	-177.86	-172.08
Floor 15	52.43	236.75	294.75	-167.92	-159.45
Floor 14	49.38	223.93	278.49	-157.54	-150.48
Floor 13	46.33	211.13	261.10	-147.40	-142.54
Floor 12	43.28	197.20	243.55	-136.91	-130.20
Floor 11	40.23	183.07	226.58	-126.71	-117.74
Floor 10	36.58	164.60	204.56	-113.81	-103.08
Floor 9	32.92	146.41	181.16	-101.57	-90.08
Floor 8	29.26	127.98	157.27	-89.20	-79.80
Floor 7	25.60	109.84	133.05	-77.19	-70.07
Floor 6	21.95	91.59	108.63	-65.18	-59.66
Floor 5	18.29	73.92	84.87	-53.40	-47.55
Floor 4	14.63	57.19	62.66	-42.18	-35.94
Floor 3	10.97	42.02	43.00	-31.28	-26.02
Floor 2	7.32	27.94	25.88	-21.05	-16.67
Floor 1	3.66	15.03	11.98	-12.03	-8.37
Plinth	0.00	4.85	2.58	-3.94	-1.68
Base	-3.81	0.00	0.00	0.00	0.00

Figure 3.10: P 80000 kN-s/m C2 y-axis Deformed Shape

Figure 3.11: P 80000 kN-s/m C2 x-axis Deformed Shape

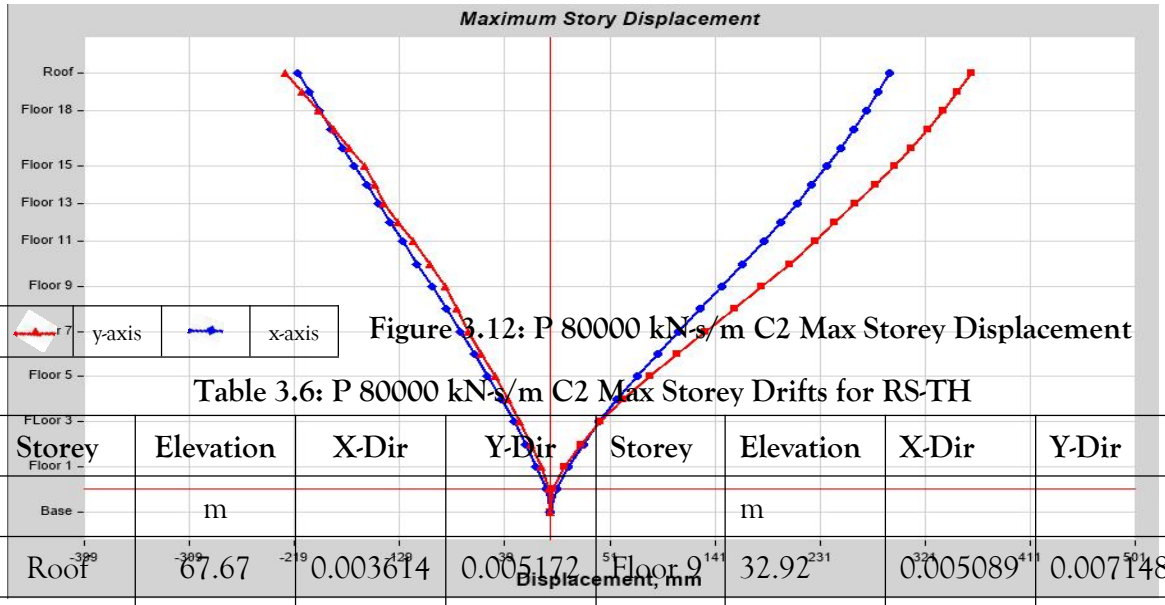

Figure 3.12: P 80000 kN-s/m C2 Max Storey Displacement

Table 3.6: P 80000 kN-s/m C2 Max Storey Drifts for RS-TH

Storey	Elevation	X-Dir	Y-Dir	Storey	Elevation	X-Dir	Y-Dir
	m				m		
Roof	67.67	0.003614	0.005172	Floor 9	32.92	0.005089	0.007148
Floor 19	64.62	0.003766	0.005361	Floor 8	29.26	0.005082	0.007084
Floor 18	61.57	0.004079	0.005634	Floor 7	25.60	0.005027	0.00683
Floor 17	58.52	0.004222	0.005864	Floor 6	21.95	0.004831	0.006643
Floor 16	55.47	0.004477	0.00594	Floor 5	18.29	0.004576	0.006146
Floor 15	52.43	0.004389	0.00589	Floor 4	14.63	0.00418	0.005407
Floor 14	49.38	0.004678	0.006013	Floor 3	10.97	0.003882	0.004716
Floor 13	46.33	0.004775	0.006172	Floor 2	7.32	0.003528	0.003801
Floor 12	43.28	0.004943	0.006661	Floor 1	3.66	0.002847	0.002583
Floor 11	40.23	0.005103	0.007163	Plinth	0.00	0.001276	0.000712
Floor 10	36.58	0.005136	0.007341	Base	-3.81	0	0

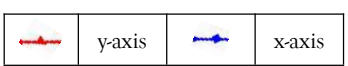

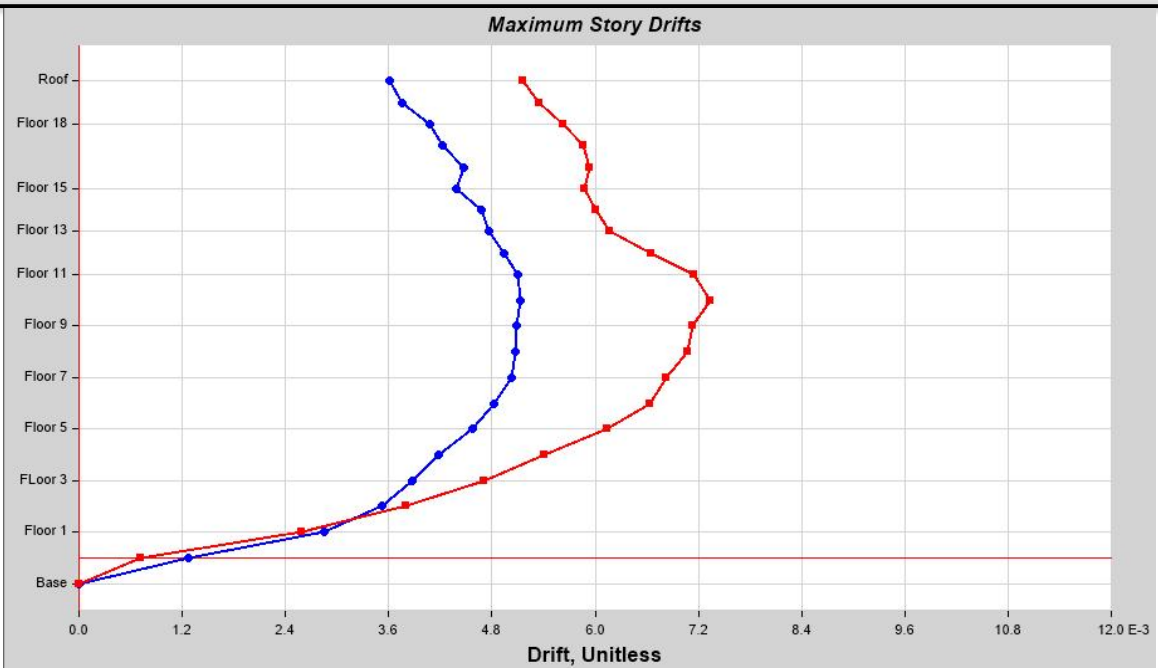

Figure 3.13: P 80000 kN-s/m C2 Inter-Storey

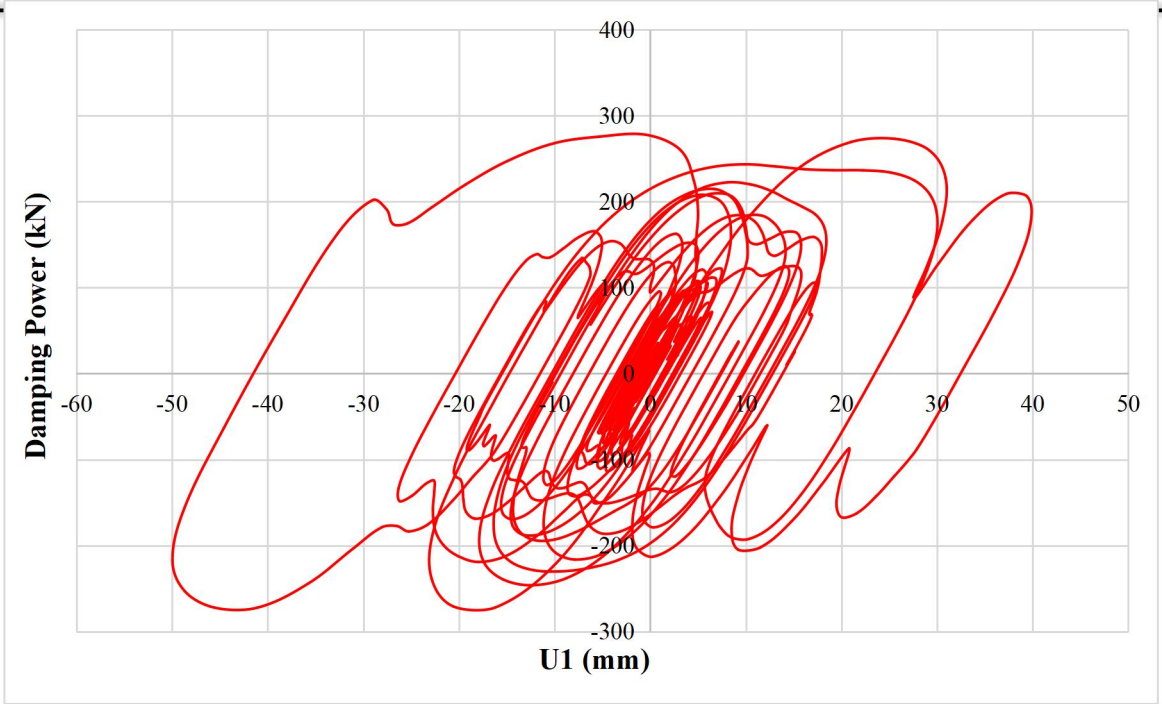

Figure 3.14: P 80000 kN-s/m C2 Hysteresis Plot

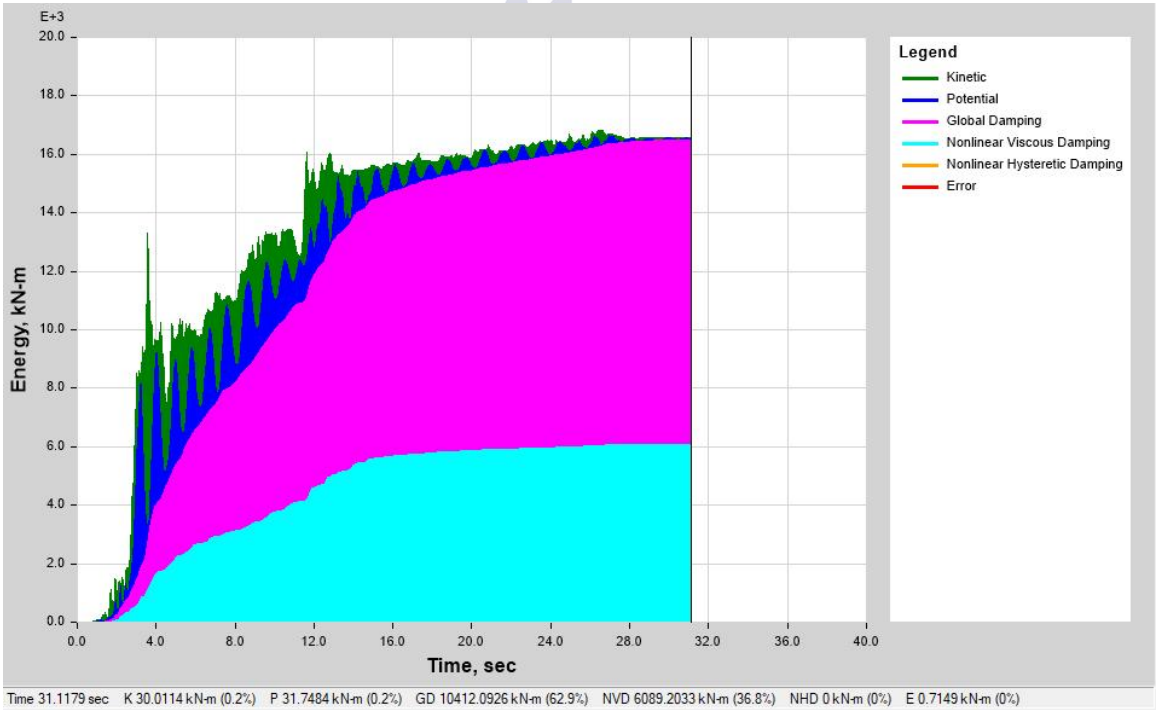

Figure 3.15: P 80000 kN-s/m C2 Cumulative Energy Plot

3.3.3 P. 80000kN-s/m Combination 3 (C3):

- 40 Wall Mounted Viscous Dampers applied on each side of the building from Plinth to 20th Floor.
- C3's Max Storey Displacements are x-axis 265.37 mm and y-axis is 314.37 mm; Max inter-storey drift is 0.006179. Hysteresis plot is also acceptable.
- Max Non-Linear Viscous Damping is 58.6%.

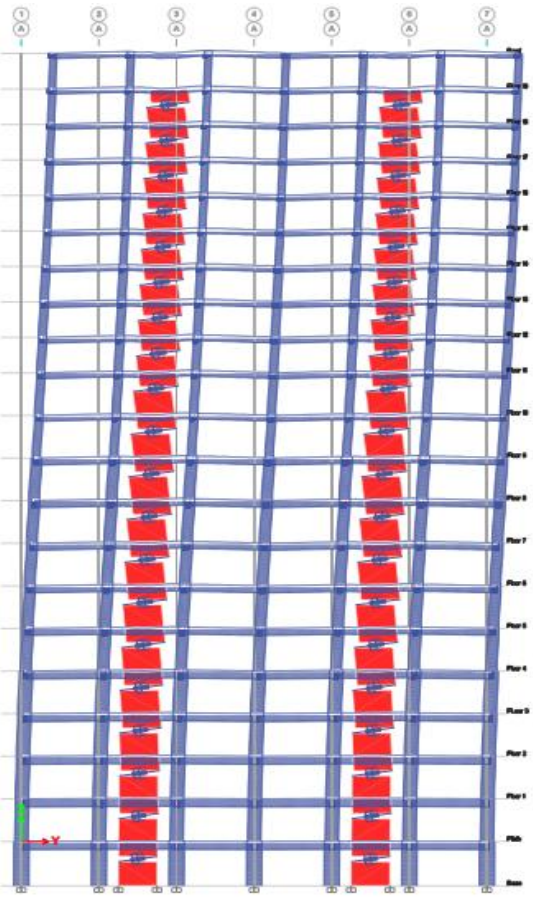

Figure 3.16: P 80000 kN-s/m C3 y-axis Deformed Shape

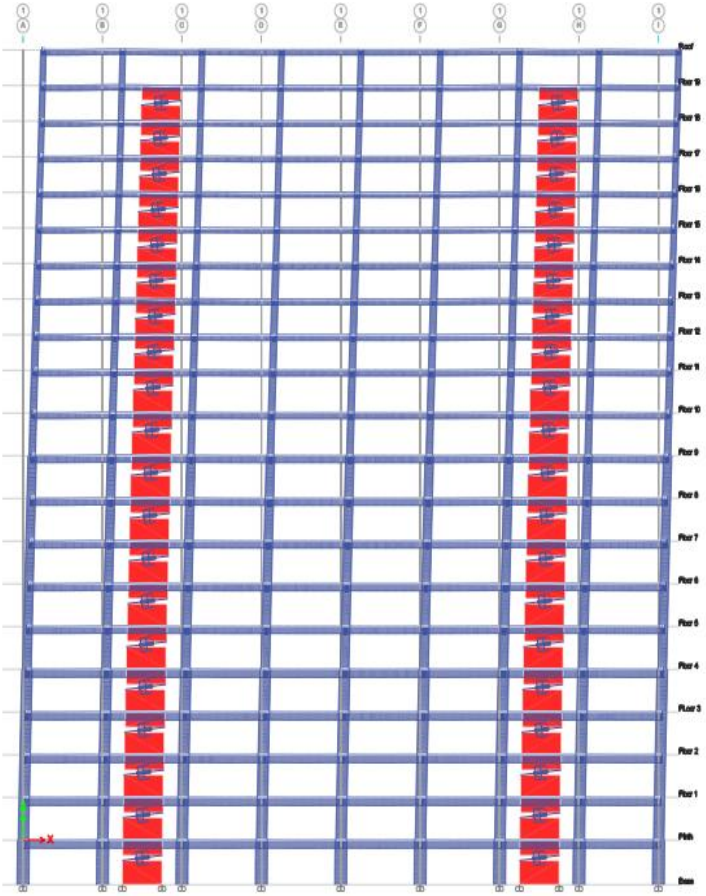

Figure 3.17: P 80000 kN-s/m C3 X-axis Deformed Shape

Table 3.7: P 80000 kN-s/m C3 Max and Min Storey Displacements for RS-TH

Storey	Elevation	X-Dir	Y-Dir	X-Dir Min	Y-Dir Min
	m	mm	mm	mm	mm
Roof	67.67	265.37	314.37	0.00	0.00
Floor 19	64.62	257.17	322.23	-186.91	-131.36
Floor 18	61.57	248.10	312.53	-177.87	-124.84
Floor 17	58.52	238.59	301.58	-168.46	-118.37
Floor 16	55.47	228.56	289.56	-159.03	-111.69
Floor 15	52.43	218.01	276.78	-149.36	-104.79

Floor 14	49.38	206.75	262.00	-139.68	-97.62
Floor 13	46.33	195.18	246.71	-129.80	-90.31
Floor 12	43.28	182.98	230.44	-119.84	-82.83
Floor 11	40.23	170.31	212.49	-108.66	-75.18
Floor 10	36.58	154.09	192.26	-97.67	-66.22
Floor 9	32.92	137.21	168.21	-85.95	-57.31
Floor 8	29.26	120.30	145.65	-74.37	-48.53
Floor 7	25.60	103.25	122.88	-62.98	-39.97
Floor 6	21.95	86.43	100.36	-52.16	-30.93
Floor 5	18.29	70.16	80.04	-41.95	-21.18
Floor 4	14.63	54.55	60.15	-32.02	-12.68
Floor 3	10.97	39.98	43.25	-21.05	-6.42
Floor 2	7.32	26.47	28.02	-10.91	-4.00
Floor 1	3.66	14.38	15.90	-3.09	-1.26
Plinth	0.00	4.75	4.78	0.00	0.00
Base	-3.81	0.00	0.00	0.00	0.00

Figure 3.18: P 80000 kN-s/m C3 Max Storey Displacement

Table 3.8: P 80000 kN-s/m C3 Max Storey Drifts for RS-TH

Storey	Elevation	X-Dir	Y-Dir	Storey	Elevation	X-Dir	Y-Dir
	m				m		
Roof	67.67	0.002924	0.003382	Floor 9	32.92	0.004627	0.006101
Floor 19	64.62	0.003072	0.003511	Floor 8	29.26	0.004658	0.005991
Floor 18	61.57	0.003204	0.003773	Floor 7	25.60	0.004599	0.005757
Floor 17	58.52	0.00335	0.004101	Floor 6	21.95	0.004444	0.005381
Floor 16	55.47	0.003498	0.004461	Floor 5	18.29	0.004291	0.004869
Floor 15	52.43	0.003724	0.004847	Floor 4	14.63	0.003968	0.004239
Floor 14	49.38	0.003818	0.005083	Floor 3	10.97	0.003675	0.003597
Floor 13	46.33	0.004034	0.005371	Floor 2	7.32	0.003279	0.002755
Floor 12	43.28	0.004198	0.005639	Floor 1	3.66	0.002599	0.001656
Floor 11	40.23	0.004461	0.005817	Plinth	0.00	0.001241	0.000448
Floor 10	36.58	0.00465	0.006179	Base	-3.81	0	0

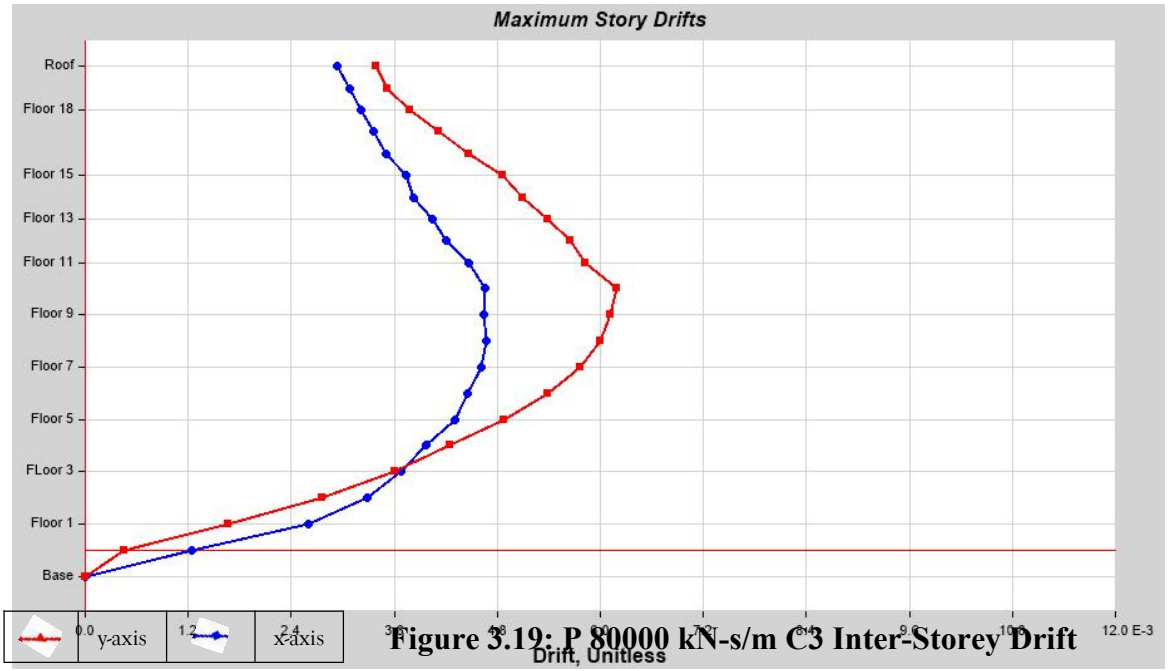

Figure 3.19: P 80000 kN-s/m C3 Inter-Storey Drift

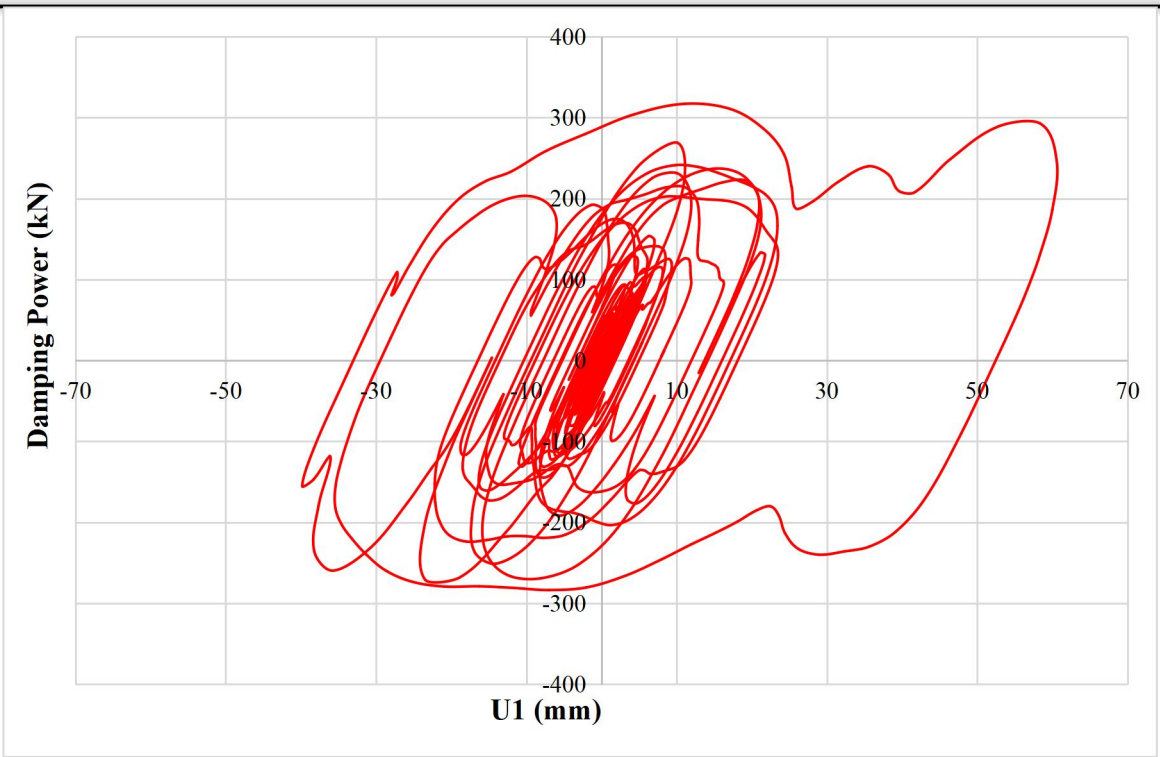

Figure 3.20: P 80000 kN-s/m C3 Hysteresis Plot

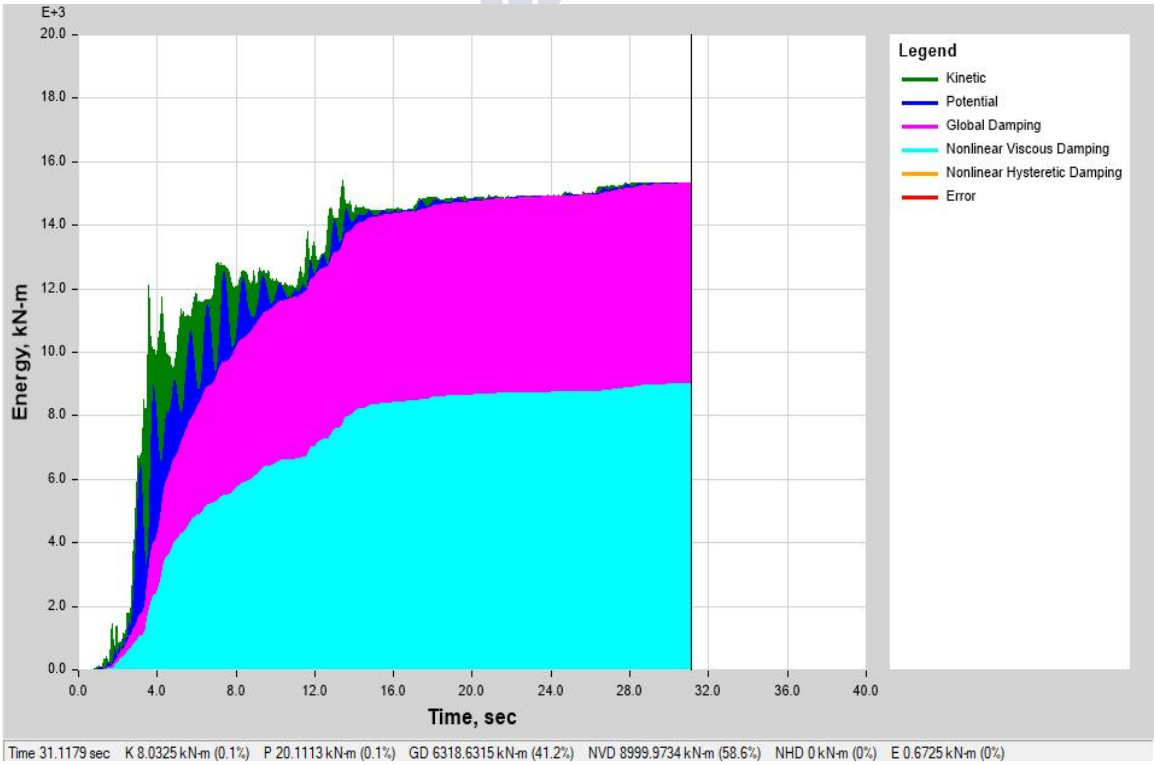

Figure 3.21: P 80000 kN-s/m C3 Cumulative Energy Plot

3.4 Result Comparison:

Model without Dampers and Models with 80000 kN-s/m Damping Power:

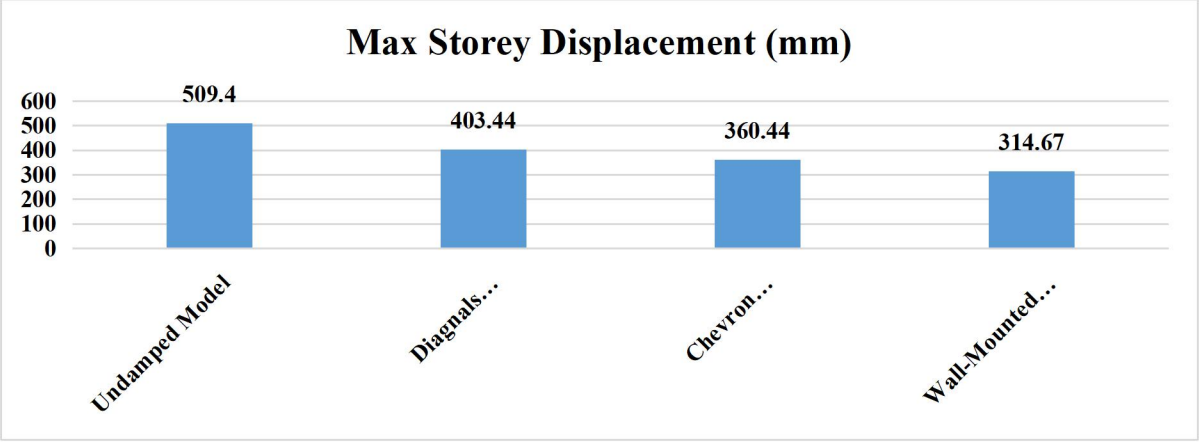

Figure 3.22: Undamped Model and Model Dampers with 80000 kN-s/m Max Storey Displacement Comparison

Figure 3.23: Undamped Model and Model Dampers with 80000 kN-s/m Max Inter-Storey Drift Comparison

Figure 3.24: Undamped Model and Model Dampers with 80000 kN-s/m Nonlinear Viscous Damping Comparison

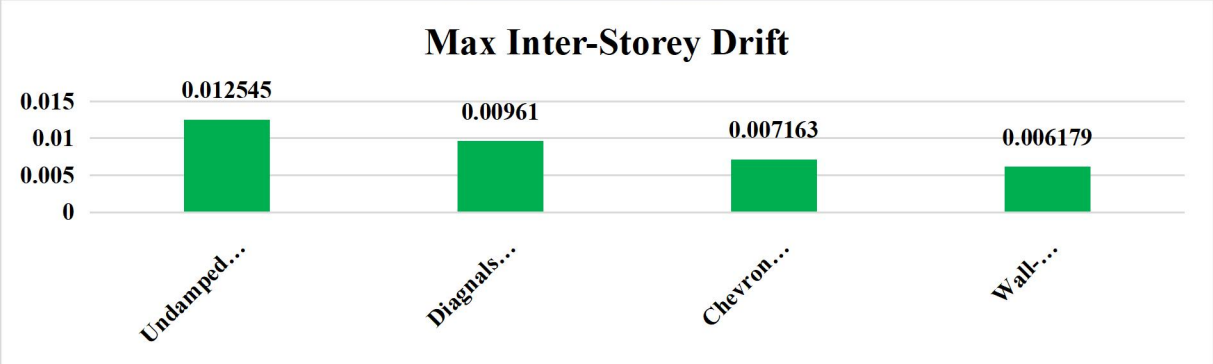

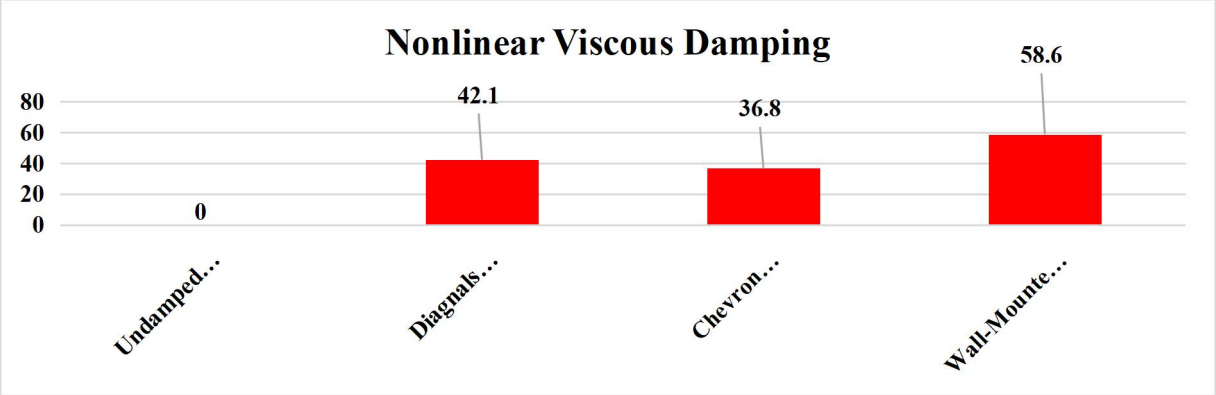

4. Conclusion

The numerical results demonstrate that fitting fluid viscous dampers (FVDs) to the 20-storey RC frame markedly improves lateral performance compared with the undamped model (max inter-storey drift ≈ 0.01157; roof displacement ≈ 509.48 mm). All three damper orientations reduce drift and displacement significantly: the chevron layout reduces peak drift to ≈0.00961 and roof motion to ≈403.44 mm while dissipating ≈42.1% of input seismic energy; the single-diagonal layout reduces drift to ≈0.00716 and roof motion to ≈360.44 mm with ≈36.8% energy dissipation; and the wall-mounted configuration gives the best seismic control, lowering drift to ≈0.00618 and roof displacement to ≈314.37 mm while dissipating ≈58.6% of the energy. Hysteresis plots corroborate these findings: the wall mounted scheme produces the largest hysteretic loop area (highest energy absorption), chevron and diagonal configurations show moderate loop areas consistent with their dissipation percentages, and the undamped frame exhibits very narrow loops indicative of predominantly elastic behavior. In terms of deformation patterns, the undamped model displays the classic single curvature (triangular) sway; adding dampers produces more distributed drift profiles chevron and diagonal braces introduce inflection points around their attachment levels and break the simple cantilever shape, while the wall mounted dampers engage lower stories more strongly and tend to flatten the overall sway curve. Taken together, the wall mounted arrangement is recommended when the primary objective is seismic drift control and maximum energy dissipation, whereas chevron or diagonal layouts are comparatively advantageous where mitigation of low-frequency wind-induced sway is important. For mixed seismic wind coastal environments (e.g., Karachi), a combined/hybrid layout concentrating wall mounted dampers where seismic control is critical and using chevron/diagonal dampers on wind exposed facades offers a balanced, practical strategy to maximize resilience under both hazards.

References

[1] Ali, M., & Moon, K. S. (2007). Structural developments in tall buildings: Current trends and future prospects. Architectural Science Review, 50(3), 205–223. https://doi.org/10.3763/asre.2007.5027

[2] Chopra, A. K. (2012). Dynamics of structures: Theory and applications to earthquake engineering (4th ed.). Prentice Hall.

[3] Constantinou, M. C., & Symans, M. D. (1992). Experimental and analytical investigation of seismic response of structures with supplemental fluid viscous dampers. Structural Design of Tall Buildings, 1(1), 1–22. https://doi.org/10.1002/tal.4320010102

[4] Fujita, K., Takewaki, I., & Yoshitomi, S. (2010). Optimal damper placement for seismic and wind response control of buildings. Journal of Structural and Construction Engineering, 75(649), 1609–1618. https://doi.org/10.3130/aijs.75.1609

[5] International Code Council. (2019). ACI 318-19: Building code requirements for structural concrete. American Concrete Institute.

[6] American Society of Civil Engineers. (2016). ASCE 7-16: Minimum design loads and associated criteria for buildings and other structures. ASCE.

[7] Hwang, J. S., & Kim, J. (2004). Performance evaluation of tall buildings with viscoelastic dampers. Engineering Structures, 26(5), 671–681. https://doi.org/10.1016/j.engstruct.2003.12.006

[8] Makris, N., & Constantinou, M. C. (1991). Fractional-derivative Maxwell model for viscous dampers. Journal of Structural Engineering, 117(9), 2708–2724. https://doi.org/10.1061/(ASCE)0733-9445(1991)117:9(2708)

Lin, P. Y., & Tsai, M. H. (2008). Seismic performance of toggle-brace-damper systems for buildings. Journal of Structural Engineering, 134(1), 56–63. https://doi.org/10.1061/(ASCE)0733-9445(2008)134:1(56)

] Lee, D., & Taylor, D. P. (2001). Viscous damper development and future trends. The Structural Design of Tall Buildings, 10(5), 311–320. https://doi.org/10.1002/tal.191

] Soong, T. T., & Dargush, G. F. (1997). Passive energy dissipation systems in structural engineering. Wiley.

] Constantinou, M. C., & Symans, M. D. (1993). Seismic response of structures with supplemental damping. The Structural Design of Tall Buildings, 2(2), 77–92. https://doi.org/10.1002/tal.4320020202

] Wu, J. C., & Hanson, R. D. (1991). Reduction of building seismic response by viscoelastic dampers. Journal of Structural Engineering, 117(1), 226–244. https://doi.org/10.1061/(ASCE)0733-9445(1991)117:1(226)

] Zhang, R. H., & Soong, T. T. (1992). Seismic design of viscoelastic dampers for structural applications. Journal of Structural Engineering, 118(5), 1375–1392. https://doi.org/10.1061/(ASCE)0733-9445(1992)118:5(1375)

] Lu, Z., & Xu, Z. D. (2016). Seismic performance evaluation of high-rise buildings with viscous dampers. Earthquake Engineering and Engineering Vibration, 15(4), 789–803.

[16] American Concrete Institute. (2019). Building code requirements for structural concrete (ACI 318-19). ACI.

] American Society of Civil Engineers. (2016). Minimum design loads and associated criteria for buildings and other structures (ASCE/SEI 7-16). ASCE.